

NCF1 (p47^{phox})-deficient chronic granulomatous disease: comprehensive genetic and flow cytometric analysis

Douglas B. Kuhns,¹ Amy P. Hsu,² David Sun,³ Karen Lau,¹ Danielle Fink,¹ Paul Griffith,³ Da Wei Huang,⁴ Debra A. Long Priel,¹ Laura Mendez,¹ Samantha Kreuzburg,² Christa S. Zerbe,² Suk See De Ravin,² Harry L. Malech,² Steven M. Holland,² Xiaolin Wu,³ and John I. Gallin²

¹Neutrophil Monitoring Laboratory, Applied/Developmental Research Directorate, Leidos Biomedical Research, Inc., Frederick National Laboratory for Cancer Research, Frederick, MD; ²Laboratory of Clinical Immunology and Microbiology, National Institute of Allergy and Infectious Diseases, National Institutes of Health, Bethesda, MD; ³Cancer Research Technology Program, Leidos Biomedical Research, Inc., Frederick National Laboratory for Cancer Research, Frederick, MD; and ⁴Lymphoid Malignancies Branch, Center for Cancer Research, National Cancer Institute, National Institutes of Health, Bethesda, MD

Key Points

- Flow cytometric analysis of p47^{phox} expression in permeabilized neutrophils quickly identifies patients and carriers of p47^{phox} CGD.
- Genomic ddPCR identifies patients and carriers of Δ GT *NCF1*, the most common mutation in p47^{phox} CGD.

Mutations in *NCF1* (p47^{phox}) cause autosomal recessive chronic granulomatous disease (CGD) with abnormal dihydrorhodamine (DHR) assay and absent p47^{phox} protein. Genetic identification of *NCF1* mutations is complicated by adjacent highly conserved (>98%) pseudogenes (*NCF1B* and *NCF1C*). *NCF1* has GTGT at the start of exon 2, whereas the pseudogenes each delete 1 GT (Δ GT). In p47^{phox} CGD, the most common mutation is Δ GT in *NCF1* (c.75_76delGT; p.Tyr26fsX26). Sequence homology between *NCF1* and its pseudogenes precludes reliable use of standard Sanger sequencing for *NCF1* mutations and for confirming carrier status. We first established by flow cytometry that neutrophils from p47^{phox} CGD patients had negligible p47^{phox} expression, whereas those from p47^{phox} CGD carriers had ~60% of normal p47^{phox} expression, independent of the specific mutation in *NCF1*. We developed a droplet digital polymerase chain reaction (ddPCR) with 2 distinct probes, recognizing either the wild-type GTGT sequence or the Δ GT sequence. A second ddPCR established copy number by comparison with the single-copy telomerase reverse transcriptase gene, *TERT*. We showed that 84% of p47^{phox} CGD patients were homozygous for Δ GT *NCF1*. The ddPCR assay also enabled determination of carrier status of relatives. Furthermore, only 79.2% of normal volunteers had 2 copies of GTGT per 6 total (*NCF1/NCF1B/NCF1C*) copies, designated 2/6; 14.7% had 3/6, and 1.6% had 4/6 GTGT copies. In summary, flow cytometry for p47^{phox} expression quickly identifies patients and carriers of p47^{phox} CGD, and genomic ddPCR identifies patients and carriers of Δ GT *NCF1*, the most common mutation in p47^{phox} CGD.

Introduction

Chronic granulomatous disease¹ is caused by defects in any 1 of 5 subunits of the phagocyte nicotinamide adenine dinucleotide phosphate (NADPH) oxidase (phox). In the Western world, defects in p47^{phox} account for 25% of chronic granulomatous disease (CGD) patients, second only to gp91^{phox} as a cause of CGD.² However, in the Middle East and India,³⁻⁵ where consanguineous marriage are more common, defects in p47^{phox} are often a more frequent cause of CGD compared with gp91^{phox}. CGD is characterized by a failure of phagocytes (neutrophils, monocytes, macrophages, and eosinophils) to generate superoxide anion radical (O₂^{•-}) and other related reactive oxygen species (ROS), leading to recurrent infections, inflammation, and increased mortality.⁶ Phorbol ester induces ROS production in vitro, which can be quantitated by ferricytochrome c reduction, luminol-enhanced chemiluminescence, or

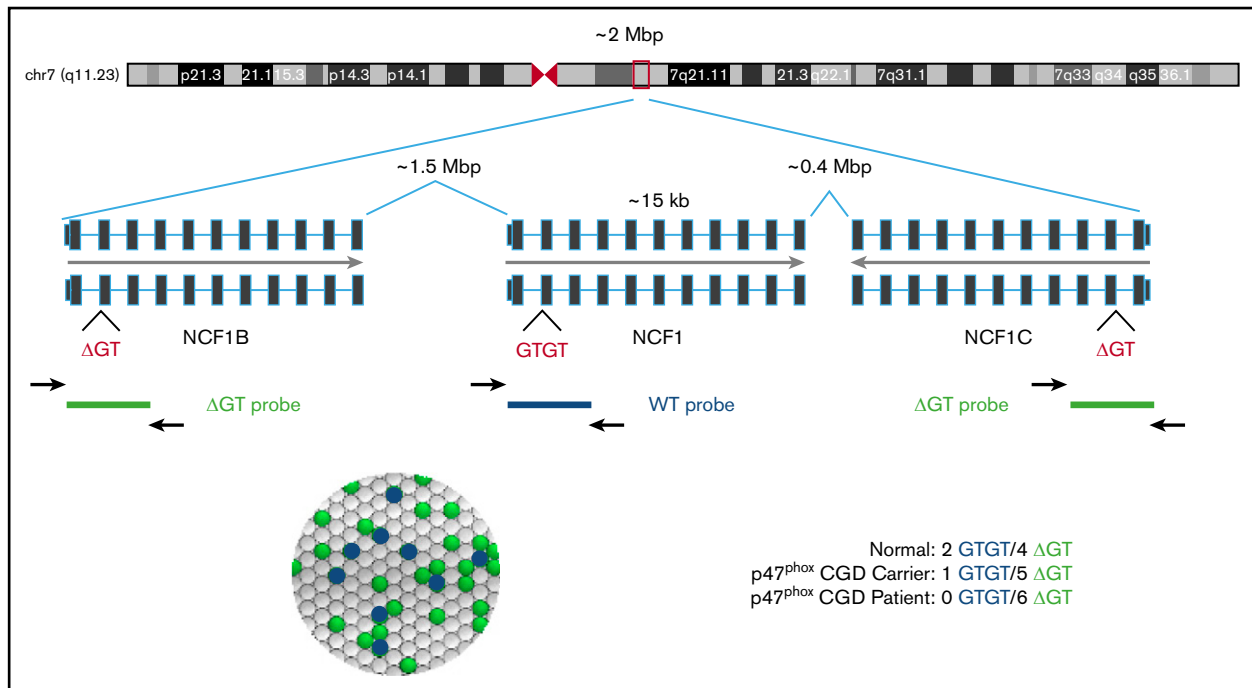


Figure 1. Analysis of *NCF1* by ddPCR. Two distinct probes (one that recognizes the GTGT [blue] found in *NCF1* and a second that recognizes the ΔGT [green] found in *NCF1B* and *NCF1C*) were added to diluted genomic DNA. A 20-μL PCR mixture was dispersed into 20 000 oil-coated nanodroplets, and PCR was performed. The droplets were analyzed to determine the number of “Blue” and “Green” nanodroplets. The image at the bottom left depicts the bead distribution of the ddPCR reaction. The clear beads represent beads without GTGT or ΔGT sequences, and therefore have no amplified probe or color. The blue beads represent beads containing a GTGT sequence and PCR amplification of the GTGT-specific probe. The green beads represent beads containing a ΔGT sequence and PCR amplification of the ΔGT-specific probe. Although the DNA has been diluted to minimize the number of double-colored droplets, they do occur and are included in the analysis. However, they are detected in independent channels and, therefore, do not affect the results. The text at the bottom right depicts the possible sequences in the example in the top of the panel. Because a total of 6 alleles were expected, normal subjects were predicted to yield 2 GTGT/4 ΔGT, p47^{phox} carriers were predicted to yield 1 GTGT/5 ΔGT, and patients with p47^{phox} CGD were predicted to yield 0 GTGT/6 ΔGT.

ROS-mediated dihydrorhodamine (DHR) oxidation, detected using flow cytometry. In general, neutrophils from CGD patients exhibit very little ROS production. However, neutrophils from patients with p47^{phox} CGD have residual ROS production⁷ that is associated with a more favorable clinical course.² On DHR assay, p47^{phox} CGD neutrophils have a broad population of low ROS-producing cells. Although these clinical laboratory findings suggest the diagnosis of p47^{phox} CGD, they are not specific. The definitive diagnosis is based on immunoblotting for p47^{phox} or detection of specific mutations. These approaches cannot reliably identify clinically asymptomatic, autosomal recessive carriers of p47^{phox} CGD, complicating genetic counseling and leaving important questions about etiology and mechanism unanswered.⁸

Identification of the specific mutations in *NCF1*⁹ is complicated by highly homologous (>98%) pseudogenes (differences identified in supplemental Table 1) that are thought to have arisen through gene duplication.⁸ Wild-type *NCF1* gene has a GTGT at the start of exon 2, whereas the pseudogenes (*NCF1B* and *NCF1C*) have only a single GT (ΔGT). We developed a rapid, flow cytometer-based assay for p47^{phox} expression in permeabilized whole-blood neutrophils to phenotypically identify both p47^{phox} CGD patients and carriers. To address the genetic mechanisms, we developed a novel droplet digital polymerase chain reaction (ddPCR) assay to calculate the relative number of GTGT copies (in genomic DNA, typically 2) compared with ΔGT

copies (typically 4) and the copy number variation (CNV) at the *NCF1* locus to genotypically identify ΔGT p47^{phox} CGD patients and carriers. These assays provide tools to diagnose autosomal carriers of p47^{phox} CGD

Methods

Protocol numbers for patients and normal subjects

Heparinized bloods from both normal subjects and patients with CGD were drawn after documented informed consent in accordance with the Declaration of Helsinki under the Frederick Research Donor Program Protocol OH99-C-N046 and National Institutes of Health (NIH) protocols 93-I-0119, 07-I-0033, 95-I-0066, and 05-I-0213. To augment the diversity within our DNA cohort, an additional 75 anonymous DNAs from Asian, African American, and Hispanic individuals were obtained from a commercial supplier (BioServe Biotechnologies Ltd, Beltsville, MD)

Isolation of neutrophils and peripheral blood mononuclear cells

Peripheral blood neutrophils and mononuclear cells were harvested from diluted blood by discontinuous gradient centrifugation, as described previously.¹⁰ In general, the final preparation of neutrophils was more than 95% pure with about 4% eosinophils,

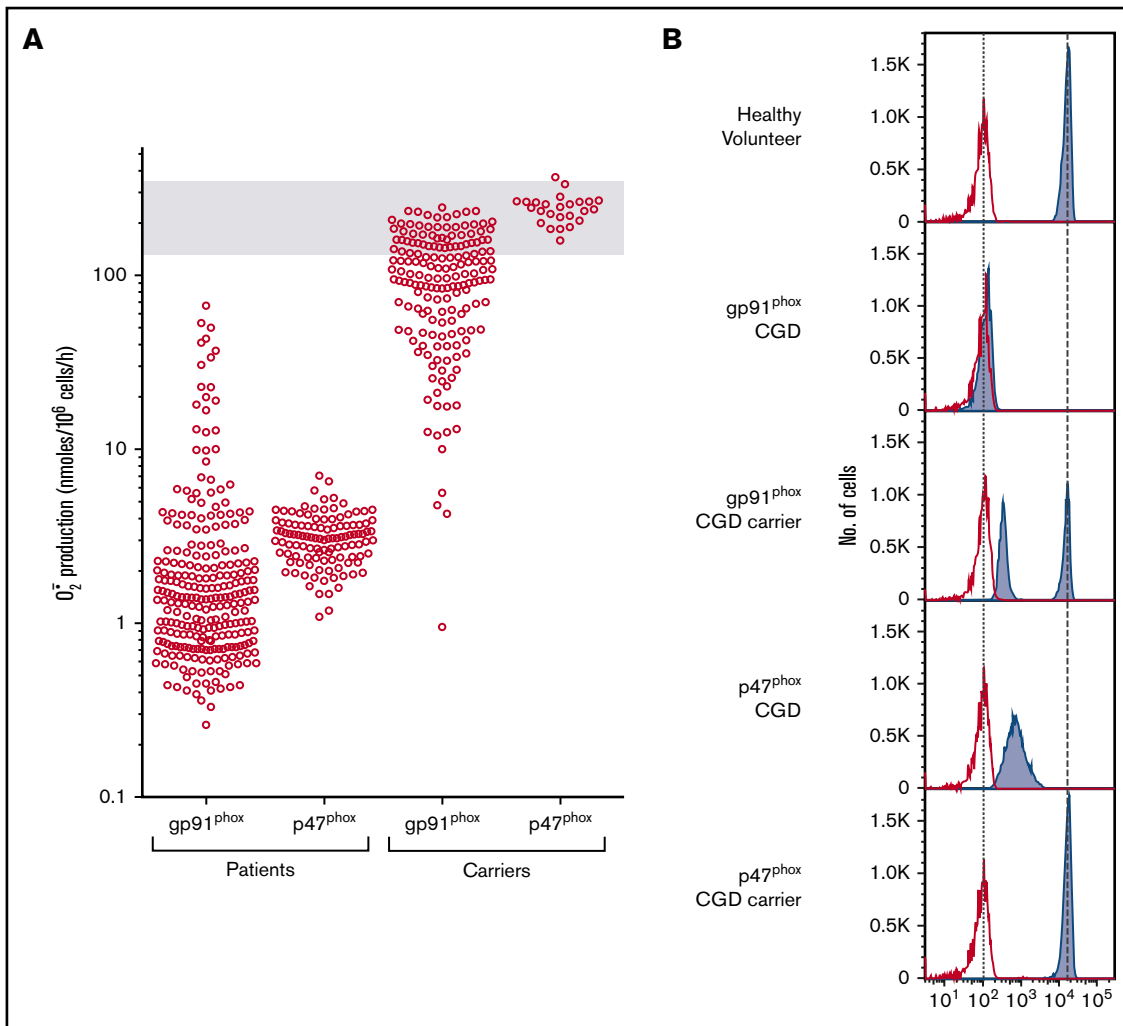


Figure 2. ROS production in patients and carriers of gp91^{phox} and p47^{phox} CGD. (A) Scatter plots represent the residual oxidase activity of phorbol 12-myristate 13-acetate (PMA)-stimulated (100 ng/mL) neutrophils isolated from individual patients and carriers of gp91^{phox} and p47^{phox} CGD determined using ferricytochrome c reduction. The region in gray is the normal range (129.9-346.3 nmoles/10⁶ cell/60 minutes) based on data from neutrophils isolated from 922 healthy volunteers (mean ± 2 standard deviation [SD]). As previously reported, neutrophils from p47^{phox} CGD patients have increased ROS production compared with most gp91^{phox} CGD patients.² Neutrophils from all carriers of p47^{phox} CGD exhibit ROS production that falls within the normal range. (B) Histograms represent the residual oxidase activity of neutrophils from patients and carriers of gp91^{phox} and p47^{phox} CGD, determined using dihydrorhodamine oxidation by flow cytometry. Neutrophil populations were gated using forward and right-angle light scattering. Open histograms represent ROS production of neutrophils treated with buffer under basal conditions; the solid gray histograms represent ROS production of neutrophils in response to PMA (400 ng/mL). The vertical dotted line represents the peak of buffer-treated neutrophils, and the vertical dashed line represents the peak of PMA-treated neutrophils.

and less than 1% monocytes and lymphocytes, as assessed by differential staining.

NADPH oxidase activity and detection of oxidase components

ROS production was measured using the dihydrorhodamine oxidation and cytochrome c reduction assays, as previously described.¹¹ A longer, 60-minute incubation with cytochrome c was found to differentiate the O₂⁻ response in patients with detectable O₂⁻ production vs patients with undetectable O₂⁻ production.⁷ Western blot analysis to determine oxidase components was performed as described.¹¹ For quantitative immunoblotting of p47^{phox}, 20 μg neutrophil lysate (Thermo Scientific Pierce BCA Protein Assay

using albumin standard) was resolved by electrophoresis and transferred to polyvinylidene difluoride membrane. The membrane was incubated overnight with goat anti-p47^{phox} (#1588) polyclonal antibody (provided by Tom Leto and Harry Malech, National Institute of Allergy and Infectious Diseases, NIH, diluted 1:1000). The membrane was incubated with donkey anti-goat secondary antibody (Abcam, diluted 1:20 000) for 1 hour. Enhanced chemiluminescence substrate (Clarity Western ECL Substrate, Bio-Rad) was added to develop p47^{phox}. Equal regions were drawn around each band, and pixel density/area was analyzed using Image Laboratory software (Bio-Rad). The blot was stripped and probed with mouse anti-actin (Millipore, diluted 1:5000). Actin was quantitated similarly and used to normalize the protein loading.

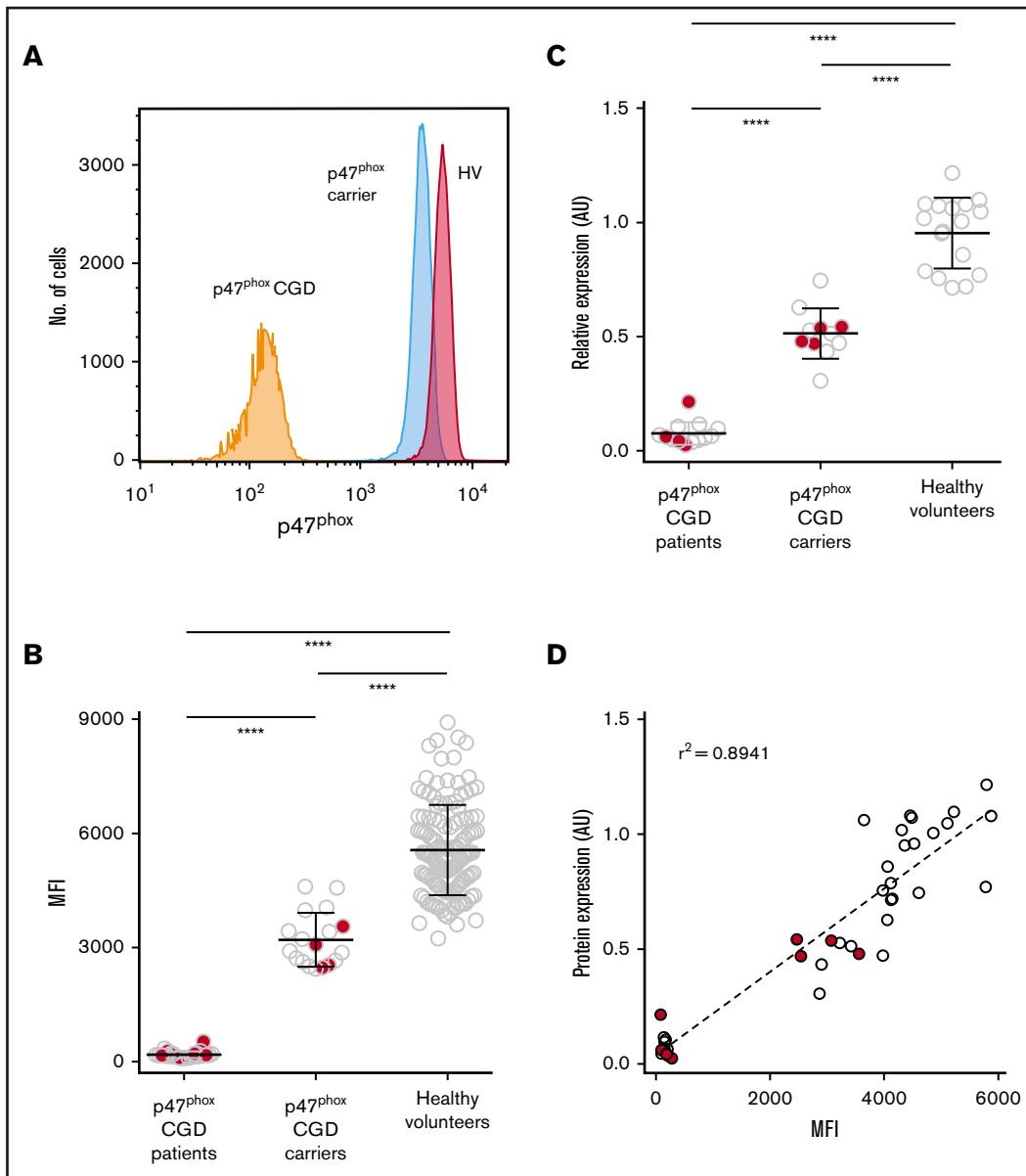


Figure 3. Quantitative analysis of p47^{phox} expression by FACS analysis and immunoblotting. To determine p47^{phox} expression, whole blood was permeabilized/fixed and then stained with anti-p47^{phox} antibody. Neutrophils were gated using forward and right-angle light scatter. The level of p47^{phox} expression on neutrophils is presented as the mean fluorescence intensity (MFI). (A) Relative histograms of a p47^{phox} CGD patient, a p47^{phox} CGD carrier, and a healthy volunteer. Summary data of the different populations are presented as scatter plots (B, C). Solid red circles in panels B, C, and D represent p47^{phox} patients and carriers with non- Δ GT mutations in *NCF1*. (C) A subset of patients and carriers of p47^{phox} CGD and healthy volunteers were analyzed for p47^{phox} expression by immunoblotting. The data for p47^{phox} expression are presented as arbitrary units relative to the expression of β -actin. Neutrophil lysates from at least 2 healthy normal volunteers were analyzed on each gel, and the mean ratio of p47^{phox}: β -actin for the normal samples was set to a value of 1.0. (D) The correlation obtained from parallel studies analyzing the expression of p47^{phox} by both flow cytometry and immunoblotting. **** $P < .0001$ (1-way analysis of variance using Tukey's multiple comparison).

Flow cytometry analysis of p47^{phox} protein expression

Using modifications of the methods described by Köker et al¹² and Wada et al,¹³ 2 aliquots of EDTA whole blood (25 μ L) were mixed with Reagent 1 (100 μ L) of IntraPrep Permeabilization kit (Beckman Coulter, A07803), vortexed vigorously, and incubated at room temperature for 15 minutes. Cells were washed with phosphate-buffered saline and spun for 5 minutes at 300g. Reagent 2 (100 μ L) from IntraPrep kit was added gently without vortexing, and cells

were further incubated for 5 minutes at room temperature. Tubes were shaken slowly, and then either rabbit recombinant monoclonal anti-p47^{phox} antibody (10 μ L, Abcam [EPR13134]) or rabbit immunoglobulin G₁ monoclonal antibody (0.5 μ L, Abcam [EPR25A]) were added. Tubes were incubated for 30 minutes at room temperature, washed, and spun at 600g for 5 minutes. The supernatant fluid was decanted and AlexaFluor488-labeled goat anti-mouse immunoglobulin G (1 μ L) was added and incubated at room temperature

for 30 minutes. Cells were washed twice, pelleting the cells at 600g for 5 minutes. Cells were resuspended in 200 μ L phosphate-buffered saline/0.5% bovine serum albumin and analyzed on a BD FACSCanto II flow cytometer (BD Biosciences), gating on neutrophils using light scatter. At least 10 000 cells were analyzed in the neutrophil gate.

Genotyping with ddPCR

For analysis of the number of GTGT and Δ GT copies in *NCF1*, *NCF1B*, or *NCF1C*, a PCR reaction master mix was made as follows: 11 μ L 2X master mix for probes, 2.2 μ L 20X assay containing PCR primers and 2 distinct probes: a 6-carboxyfluorescein-containing probe that recognizes the GTGT found in *NCF1* (blue fluorescence) and a 2'-chloro-7'-phenyl-1,4-dichloro-6-carboxyfluorescein-containing probe that recognizes the Δ GT found in *NCF1B* and *NCF1C* (green fluorescence) and 7.8 μ L H₂O (sequences of the probes used are listed in supplemental Table 2). An aliquot (21 μ L) of PCR master mix was added to each reaction well in 96-well plate or strip tubes, and then 1 μ L genomic DNA was added to each well/tube. Input genomic DNA was diluted to 5 to 20 ng/ μ L in either water or TrisEDTA (low EDTA-TE) for optimal detection. Reaction mix (20 μ L) was transferred to the sample well of a BioRad DG8 cartridge. Oil (70 μ L) was added to the BioRad QX-100 droplet generator to generate the oil-enclosed reaction droplets. Droplets (40 μ L) were transferred to an Eppendorf Twin.tec semiskirted 96-well PCR plate, and the plate was sealed. PCR reaction was performed on a BioRad T100 thermal cycler under the following conditions: 95°C for 10 minutes, 94°C for 30 seconds, 60°C for 60 seconds for 40 cycles, ramp rate 2°C/s, followed by 98°C for 10 minutes, and then held at 4°C. The plate was read on a BioRad QX200 droplet reader, and the data were analyzed using BioRad QuantaSoft 1.5 to determine the number of blue GTGT and green Δ GT droplets. Data were expressed as the proportional fraction of GTGT droplets (ie, the number of GTGT droplets divided by sum [GTGT + Δ GT] droplets) or a proportional fraction of the Δ GT droplets (ie, the number of Δ GT droplets divided by sum [GTGT + Δ GT] droplets; Figure 1). This assay simply quantitates GTGT and Δ GT sequences, regardless of whether these sequences are within their respective genes or within "fusion" genes that result from DNA recombination.^{14,15} Despite the diversity of possible gene products, the ddPCR data are sufficient to segregate the patients, carriers, and kindred in most p47^{phox} CGD families. Advanced technologies such as multiplex ligation-dependent probe amplification are required to delineate the specific *NCF1* defect.

A second ddPCR reaction was used to determine the number of *NCF1/NCF1B/NCF1C* copies relative to the single-copy gene, telomerase reverse transcriptase (*TERT*). Sequences of the probes used for the invariant region of exon 11 of *NCF1* are listed in supplemental Table 2; probes used for the *TERT* gene were proprietary and obtained from Thermo Fisher Scientific (Waltham, MA). Multiplying the proportional fraction of GTGT droplets by the total number of *NCF1/NCF1B/NCF1C* copies yields the total number of GTGT-containing copies; similarly, multiplying the proportional fraction of Δ GT droplets by the total number of *NCF1/NCF1B/NCF1C* copies yields the total number of Δ GT-containing copies. Because a total of 6 copies of *NCF1/NCF1B/NCF1C* are expected, normal subjects are predicted to have 2 GTGT copies vs 4 Δ GT copies expressed as 2/(2+4) or 2/6; autosomal recessive p47^{phox} carriers are predicted to have 1 GTGT copy and 5 Δ GT

Table 1. Representative ddPCR analyses of NCF1 in gDNA from normal subjects and CGD patients and carriers

Row	Diagnosis (a priori)	No. of GTGT droplets	No. of Δ GT droplets	GTGT/(GTGT + Δ GT)	Δ GT/(GTGT + Δ GT)	No. of NCF1/NCF1B/NCF1C droplets	No. of TERT droplets	Total NCF1/NCF1B/NCF1C copies	No. of GTGT copies	No. of Δ GT copies	GTGT copies/(GTGT + Δ GT)	Predicted genotype
1	Normal	724	1416	0.34	0.66	271	92	5.9	2.0	3.9	2/6	—
2	Normal	212	436	0.33	0.67	212	74	5.7	1.9	3.9	2/6	—
3	Normal	362	358	0.50	0.50	201	70	5.7	2.8	2.8	3/6	—
4	Normal	535	267	0.67	0.33	227	78	5.9	3.9	2.0	4/6	—
5	Normal	555	1357	0.29	0.71	502	140	7.2	2.1	5.1	2/7	—
6	p47 ^{phox} CGD	0	1080	0.00	1.0	5290	1793	6.0	0.0	6.0	0/6	Homozygous Δ GT mutation
7	p47 ^{phox} CGD	0	2640	0.00	1.0	1921	637	6.0	0.0	6.0	0/6	Homozygous Δ GT mutation
8	p47 ^{phox} CGD	852	4340	0.16	0.84	862	268	6.4	1.1	5.4	1/6	Compound heterozygous for Δ GT and non- Δ GT mutations
9	p47 ^{phox} CGD	843	1731	0.33	0.67	127	42	6.0	2.0	4.1	2/6	Non- Δ GT mutation(s)
10	Obligate p47 ^{phox} carrier	429	2098	0.17	0.83	226	79	5.7	1.0	4.8	1/6	Heterozygous Δ GT mutation
11	Obligate p47 ^{phox} carrier	646	1144	0.36	0.64	215	70	6.1	2.2	3.9	2/6	Het non- Δ GT mutation

copies, or 1/6; and p47^{phox} CGD patients are predicted to have 0 GTGT copies and 6 ΔGT copies, or 0/6.

PacBio sequencing and data analysis

A PacBio cDNA library derived from mRNA isolated from patient EBV-transformed B cells was prepared using the PacBio standard 2 kb template preparation protocol. After sequencing by PacBio RS II, circular consensus sequence reads were generated by the SMRT Analysis software with default parameters. The sequence alignment was performed by Burrows-Wheeler Aligner software; mutations were identified using VarScan 2.

Results

ROS production by p47^{phox} patients and carriers

The laboratory CGD diagnosis is based on abnormal phagocyte ROS production. ROS production in neutrophils from patients with p47^{phox} CGD is slightly increased compared with most other subtypes of CGD, but still markedly lower than normal.² The residual oxidase activities of patients with p47^{phox} CGD, measured by O₂⁻-dependent ferricytochrome c reduction, are concentrated in the upper half of the NIH CGD cohort (Figure 2A). In an earlier study CGD patients' residual neutrophil oxidase activity correlated with prognosis. Patients were grouped into 4 quartiles based on residual oxidase activity (quartile 1: least residual activity; quartile 4: most residual activity) and clinical prognosis correlated with the quartile score. Most p47^{phox} CGD patients fit in either quartile 3 or quartile 4.² The higher residual ROS production in p47^{phox} CGD was also evident by DHR (Figure 2B) and is often used to guide diagnosis.

p47^{phox} in human PMNs by immunoblotting and flow cytometry

Because carriers of p47^{phox} CGD are clinically asymptomatic, we developed a flow cytometer-based protocol for intracellular detection of p47^{phox} in polymorphonuclear neutrophils (PMNs) from whole blood (Figure 3A). Flow cytometric analysis of p47^{phox} expression in permeabilized neutrophils from healthy volunteers, p47^{phox} CGD patients, and p47^{phox} CGD carriers resolved into 3 distinct populations, with carriers having ~60% of the expression observed in healthy volunteers (Figure 3B). Importantly, this assay appeared to be independent of the specific *NCF1* mutation, in that the protein expression from carriers of the ΔGT mutation (open circles in Figure 3B-D) was comparable to that observed in carriers of non-ΔGT mutations (solid red circles in Figure 3B-D). To validate the flow cytometric assay, parallel samples from a subset of normal subjects, affected patients, and carriers of p47^{phox} CGD were subjected to both quantitative immunoblot analysis (Figure 3C) and fluorescence-activated cell sorter (FACS) analysis for p47^{phox} detection (Figure 3C) and a correlation of the immunoblot with FACS analysis of the same samples (Figure 3D). Immunoblotting of PMN showed that carriers of p47^{phox} CGD had ~50% of the expression of p47^{phox} found in normal subjects after normalization to β-actin, whereas patients with p47^{phox} CGD exhibited little, if any, expression of p47^{phox}. Therefore, flow cytometry and immunoblotting for assessing p47^{phox} expression in healthy volunteers, p47^{phox} carriers, and p47^{phox}-affected individuals is concordant between the 2 assays (Figure 3D), with an *r*² value of 0.89. Flow cytometric analysis of p47^{phox} expression in neutrophils is a rapid assay in which fixed permeabilized neutrophils can be tested in any clinical laboratory. However, given that there is some overlap of

Table 2. Distribution of GTGT and NCF1 CNV in normal and CGD populations

	GTGT/(GTGT + ΔGT)	0/4	0/5	0/6	0/7	1/5	1/6	1/7	2/4	2/5	2/6	2/7	3/6	3/7	4/6	Total
All normals, n (%)							1 (0.4)			4 (1.6)	195 (79.2)	6 (2.4)	36 (14.7)		4 (1.6)	246
p47 ^{phox} CGD, n (%)					2 (1.5)		8 (5.9)	1 (0.8)			12 (8.9)	1 (0.7)				135
Obligate p47 ^{phox} carrier, n (%)		1 (0.7)	19 (14.1)	91 (67.4)		4 (8.7)	32 (69.6)	1 (2.2)			8 (17.4)	1 (2.2)				46
p47 ^{phox} kindred, n (%)					1 (10.0)		4 (40.0)				5 (50.0)					10
Other CGD patients, carriers, and kindred, n (%)									4 (1.4)	214 (77.3)	1 (0.4)	53 (19.1)	1 (0.4)	4 (1.4)		277

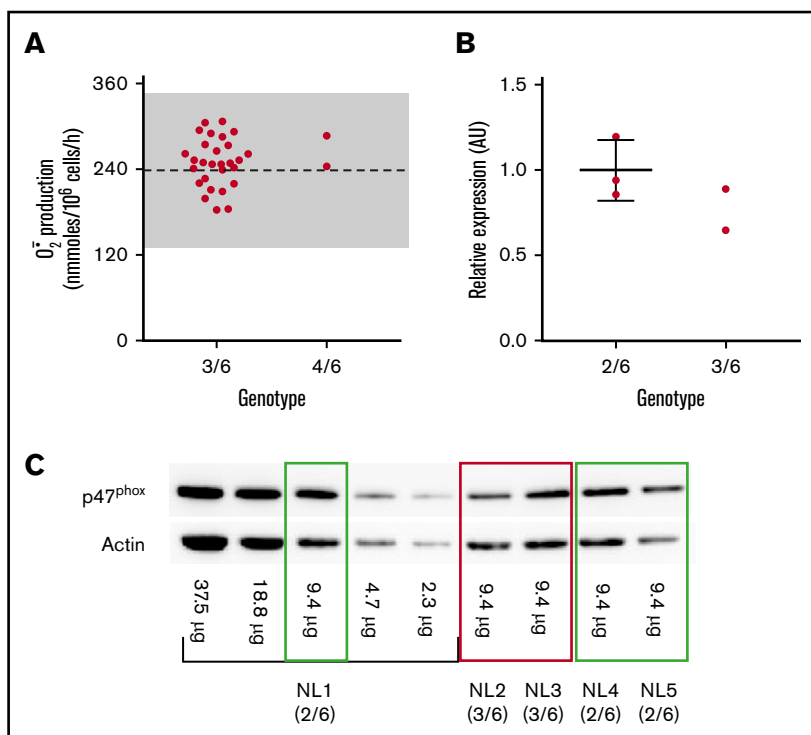


Figure 4. ROS production and p47^{phox} expression in normal subjects with increased GTGT copy number. (A) Neutrophils from healthy volunteers with increased GTGT copy number (9 with 3/6 and 1 with 4/6) exhibit normal, PMA-stimulated, neutrophil O₂⁻ production (shaded area, 238.1 ± 108.2 [mean ± 2 SD], n = 922), detected using ferricytochrome c reduction. (B-C) Neutrophils from healthy volunteers were analyzed for p47^{phox} expression. (B) Scatter plots represent neutrophil p47^{phox} expression normalized to cellular actin of 2 healthy volunteers with increased copy number of GTGT (3/6, outlined in red in panel C) comparable to that observed in neutrophils from healthy volunteers with 2/6 GTGT (outlined in green).

p47^{phox} expression by flow cytometry between healthy volunteers and p47^{phox} CGD carriers, ddPCR and immunoblotting, as shown in Figure 3C, although more labor intensive and time consuming, can provide additional robustness to the final diagnosis.

ddPCR characterization of NCF1

To circumvent the sequencing challenges of *NCF1*, we developed a pair of ddPCR assays. One assay contains probes for the intact, wild-type GTGT (found in *NCF1*) and ΔGT (found in *NCF1B* and *NCF1C*) and determines their relative distribution in a genomic DNA sample. Because these probes exclude each other, these data are presented as the proportional ratio of GTGT and ΔGT copies found within the total number of GTGT + ΔGT copies (presumed to represent the sum *NCF1*, *NCF1B*, and *NCF1C* copies). When performed on genomic DNA from most normal subjects analyzed and shown in rows 1 and 2 of Table 1, the proportional ratio of GTGT/(GTGT + ΔGT) yields values of ~0.33, which is equivalent to the expected 2 GTGT copies and 4 ΔGT copies.

A second ddPCR assay used a probe for an invariant region in exon 11 of *NCF1* common to all 3 *NCF1* genes/pseudogenes, and a second probe recognizing *TERT* to determine the number of copies of *NCF1* and its pseudogenes, collectively referred to as *NCF1/NCF1B/NCF1C*. The copy number of the normal subjects in rows 1 and 2 of Table 1 was 6 copies of *NCF1/NCF1B/NCF1C*/2 copies of *TERT*. Unexpectedly, ddPCR analysis of some normal subjects found a significant proportion (16.3%) with more than 2 copies of GTGT: 36 (14.6%) of 246 individuals had 3 GTGT copies (Table 1, row 3, and Table 2 [summary data]) and 4 (1.6%) individuals had 4 GTGT copies (Table 1, row 4, and Table 2). Interestingly, ROS in PMNs from normal subjects with either 3/6 or 4/6 GTGT was normal (Figure 4A). In addition, analysis of p47^{phox} expression by quantitative immunoblotting found no increase in p47^{phox}

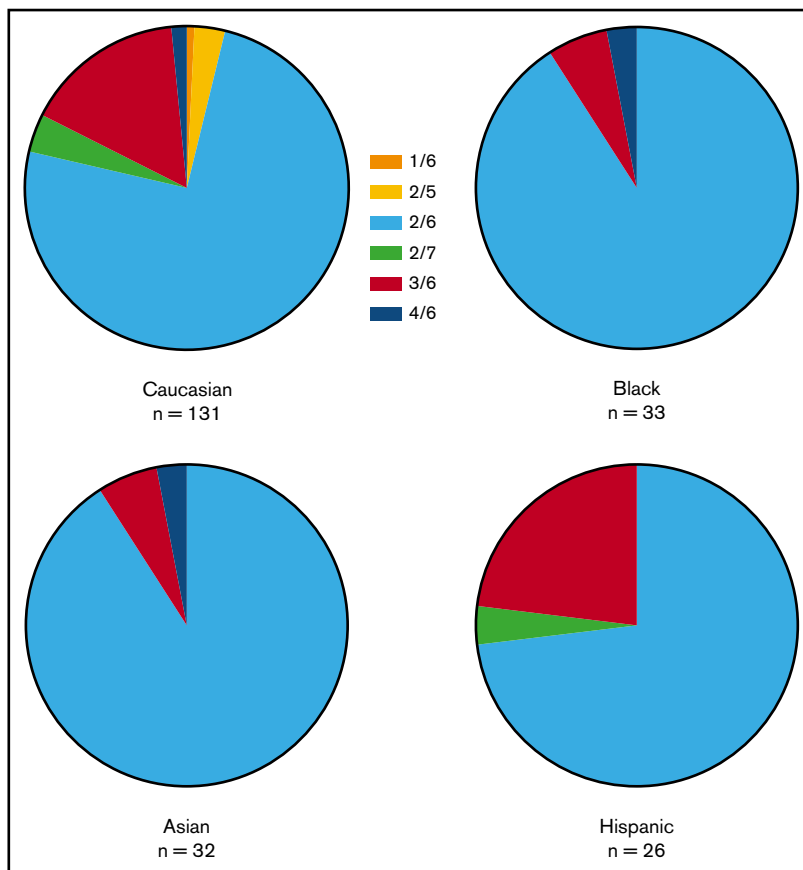
expression in PMN from 2 normal subjects with 3/6 copies of GTGT (Figure 4B). A significant number of normal subjects exhibited differences in CNV: 6 individuals had 7 copies (2.4%; Table 1, row 5, and Table 2), and 4 individuals had 5 copies (1.6%; Table 2). Overall, only 79.2% of normal control individuals exhibited the “expected” 2 copies of GTGT/6 copies of *NCF1/NCF1B/NCF1C*.

Brunson et al¹⁶ reported a significant number of Mexicans with reduced copies of *NCF1C*. Although not specifically addressed in our study, the CNV within the Hispanic population studied was comparable to that observed in the Caucasian population (Figure 5).

Figure 6 shows scatter plots of the number of GTGT copies and the number of ΔGT copies, respectively, observed in genomic DNA from normal subjects, from obligate p47^{phox} carriers (parents of p47^{phox} CGD patients and offspring of p47^{phox} CGD patients), from patients with p47^{phox} CGD, and from siblings of patients with p47^{phox} CGD, as well as other CGD patients, parents, and kindred within the NIH cohort. In the normal population, the number of GTGT copies segregated into 3 distinct clusters (2.0 ± 0.1 [n = 205], 3.0 ± 0.1 [n = 36], and 3.9 ± 0.1 [n = 4]), whereas the number of ΔGT copies segregated into 4 distinct clusters (1.9 ± 0.1 [n = 4], 3.0 ± 0.1 [n = 40], 4.0 ± 0.1 [n = 195], and 4.8 ± 0.2 [n = 7]). The normal population exhibited GTGT ratios of 2/5, 2/6, 2/7, 3/6, and 4/6. In addition, among the normal cohort studied (n = 246), 1 individual was identified as a carrier of p47^{phox} CGD, near the expected frequency of 1 in 500 based on the Hardy-Weinberg equation. In addition, the genotype frequency of CNV in the normal cohort described in this report paralleled that reported by Olsson et al.¹⁷

Most, but not all, of the p47^{phox} CGD patients studied were diagnosed based on abnormal PMA-induced DHR oxidation and p47^{phox} immunoblotting. Subsequent analysis of genomic DNA by

Figure 5. Ethnic differences in CNV in GTGT/ Δ GT distribution among healthy volunteers.



ddPCR found that 83.7% (113 patients from 88 families) of $p47^{phox}$ CGD patients within the NIH cohort were homozygous for the Δ GT mutation (0 copies GTGT; Table 1, rows 6 and 7, and Table 2); an obligate carrier of a $p47^{phox}$ CGD patient exhibited 1 copy of GTGT (Table 1, row 10). Of the remaining patients, 6.7% (9 patients from 8 families) were compound heterozygotes (1 *NCF1* carrying Δ GT and the other carrying GTGT with a mutation distinct from Δ GT; Table 1, row 8, and Table 2). Finally, 9.6%, (13 patients from 10 families) of $p47^{phox}$ CGD patients exhibited 2 copies of GTGT; they are presumed to carry 2 non- Δ GT mutations (Table 1, row 9, and Table 2); obligate carriers of these $p47^{phox}$ CGD patients exhibited 2 copies of GTGT with a presumed non- Δ GT mutation on 1 allele (Table 1, row 11, and Table 2). It should be noted that ddPCR analysis alone would have been sufficient to diagnose the patients with $p47^{phox}$ CGD who were homozygous for the Δ GT mutation (0/6); neither a DHR nor a $p47^{phox}$ immunoblot would have been necessary for the diagnosis. However, ddPCR would have been inadequate to identify those patients who were compound heterozygotes and those who were homozygous for non- Δ GT mutations; a DHR and $p47^{phox}$ expression by protein detection would have been necessary for diagnosis of $p47^{phox}$ -deficient CGD. For a patient with an abnormal DHR, ddPCR could provide a genetic diagnosis of mutations at the GTGT/ Δ GT site; in combination with a $p47^{phox}$ immunoblot or flow cytometry, it could be used to identify the more than 14% of $p47^{phox}$ CGD patients with non- Δ GT mutations.

The pedigrees of families within the NIH cohort are presented in Figure 7. The obligate carrier parents of $p47^{phox}$ CGD patients

homozygous for the Δ GT mutation were found to carry only 1 copy of GTGT (Figure 7, families A-E). Among the siblings of $p47^{phox}$ CGD patients with homozygous Δ GT mutations, ddPCR identified individuals with 2 copies of GTGT (unaffected siblings) and those with 1 copy of GTGT ($p47^{phox}$ carriers with a wild-type allele and a Δ GT allele (eg, Figure 7, families D and E). In families A-E, the CNV was invariant between the parents and children within families. Of the 90 $p47^{phox}$ CGD families with 0 copies of GTGT, patients in 74 families were 0/6 (82.2%), patients in 12 families were 0/5 (13.3%), patients in 2 families were 0/7 (2.2%), and a patient from 1 family (1.1%) was 0/4. In families F-H, the CNV did not vary among the $p47^{phox}$ CGD siblings within families; all were 0/5 (and none were 0/4 or 0/6).

Families I, J, and K, the parents and the patients, had a 2/6 genotype (Figure 7). Because these patients were diagnosed with $p47^{phox}$ CGD based on an abnormal DHR and $p47^{phox}$ immunoblot, these families are presumed to have mutations in *NCF1* distinct from the Δ GT mutations. In family I, next-generation sequencing of *NCF1* cDNA (PacBio) identified a homozygous 15 base deletion within exon 8 of *NCF1* (supplemental Figure 1), whereas the GTGT at the start of exon 2 remained intact.

In families L, M, and N, patients identified with $p47^{phox}$ CGD were analyzed by ddPCR and were found to have 1/6 or 1/7, suggesting that they are compound heterozygotes, carrying 1 GTGT allele with a mutation in *cis*, and the other allele Δ GT. In family M, ddPCR analysis of 1 obligate $p47^{phox}$ parent found 1/6, indicating a carrier of the Δ GT mutation, whereas the other parent was 2/6 and

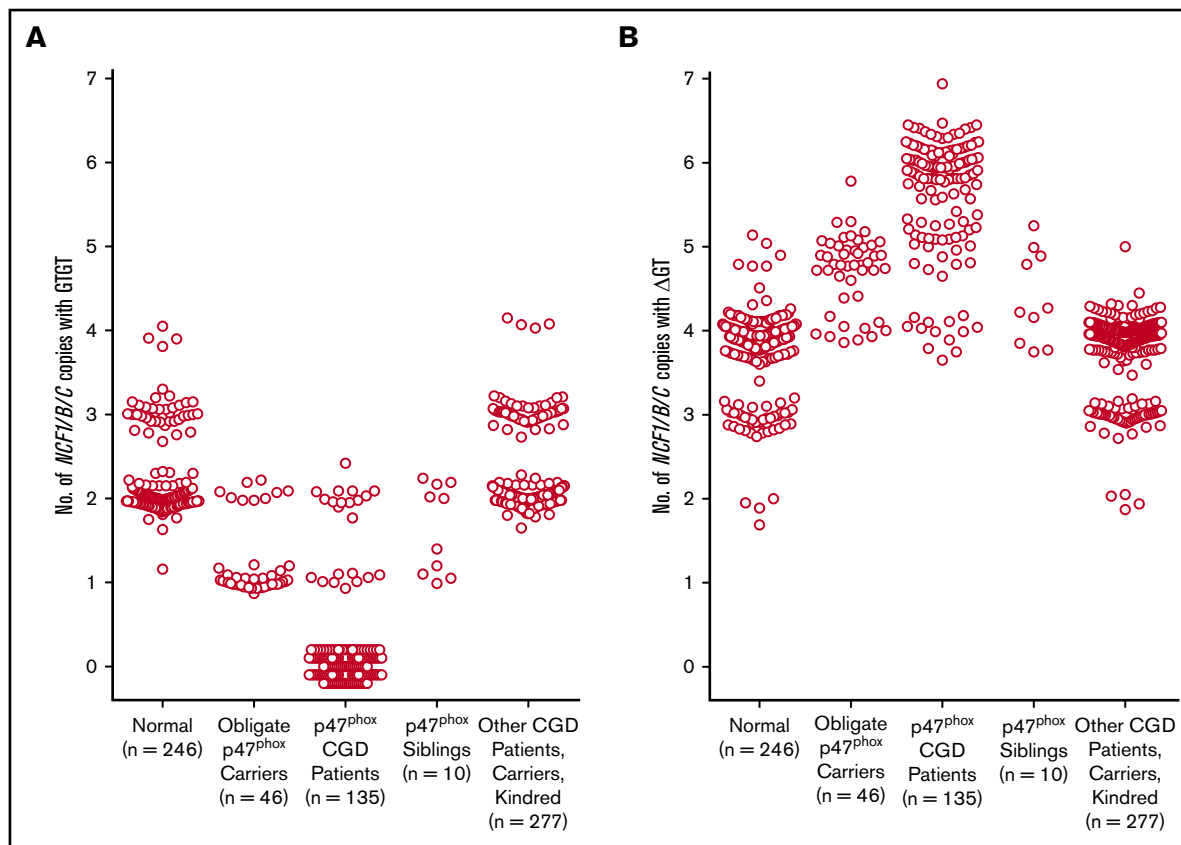


Figure 6. GTGT copies and Δ GT copies in normal subjects, p47^{phox} CGD patients, carriers, and kindred; gp91^{phox} CGD patients, carriers, and kindred; and other patients with CGD. Data from all individuals tested by ddPCR and analyzed as described in Table 2 are presented as scatter plots based on the diagnosis. (A) Number of GTGT copies. (B) Number of Δ GT copies.

presumably has another mutation in p47^{phox}. In family N, offspring of the p47^{phox} patient in the second generation presumably carries the non- Δ GT mutation.

To validate the specificity of the ddPCR among CGD patients, DNA samples from the NIH CGD cohort including patients with X-linked CGD (n = 107), their X-linked carrier mothers (n = 113), other unaffected family members, and patients, carriers, and kindred with other forms of autosomal recessive CGD were analyzed (Table 2; Figure 6). None of the individuals in this cohort (n = 277) had reduced GTGT copies. Moreover, 54 (19.5%) individuals exhibited 3 copies of GTGT and 4 (1.4%) individuals exhibited 4 copies of GTGT, similar to the findings in our normal population.

Discussion

In general, identification of the specific gene defects leading to loss of p22^{phox}, p67^{phox}, gp91^{phox}, and p40^{phox} can be easily obtained by traditional Sanger sequencing. However, identification of the specific *NCF1* genetic defects in patients with p47^{phox} CGD is complicated by the highly homologous (>98%) pseudogenes. The diagnosis is currently often made using a gene-scan protocol in which the regions of *NCF1* and its pseudogenes containing the GTGT or Δ GT are amplified by PCR, and the resultant PCR products separated by electrophoresis; the *NCF1* PCR product is 2 nucleotide base pairs longer (GTGT) than the PCR products of

NCF1B and *NCF1C* (Δ GT).¹⁸ The ratio of the peak heights of these products is used as a basis for diagnosis; normal volunteers are expected to exhibit a ratio of 2 GTGT:4 Δ GT, carriers are expected to exhibit a ratio of 1 GTGT:5 Δ G, and CGD patients are expected to exhibit only 1 Δ GT peak. This method assumes little variation in the GTGT: Δ G ratio and little variation in the numbers of *NCF1* and pseudogene copies. However, we and others have found considerable variation in the normal population, suggesting that this technique may not be as reliable as thought.¹⁷

The diagnosis of p47^{phox} CGD is generally based on clinical history followed by demonstration of an abnormal DHR and lack of mutation in any other NADPH oxidase component. Immunoblot of p47^{phox} in neutrophil lysate may take several days to complete and requires relatively large volumes of fresh blood. In contrast, our FACS assay for p47^{phox} in permeabilized PMNs is faster, is quantitative, requires less blood, and parallels those obtained by quantitative immunoblotting. This assay expands the diagnostic repertoire for carriage of p47^{phox} CGD, as carriers have only ~50% to 60% of normal expression of p47^{phox} protein in both assays. Interestingly, carriers with the Δ GT mutation and carriers with non- Δ GT mutations both demonstrate decreased levels of p47^{phox} protein. Because carriers of p47^{phox} CGD are phenotypically normal, this finding has added clinical relevance in genetic therapies, as it lowers the bar of protein needed to attain phenotypic correction.

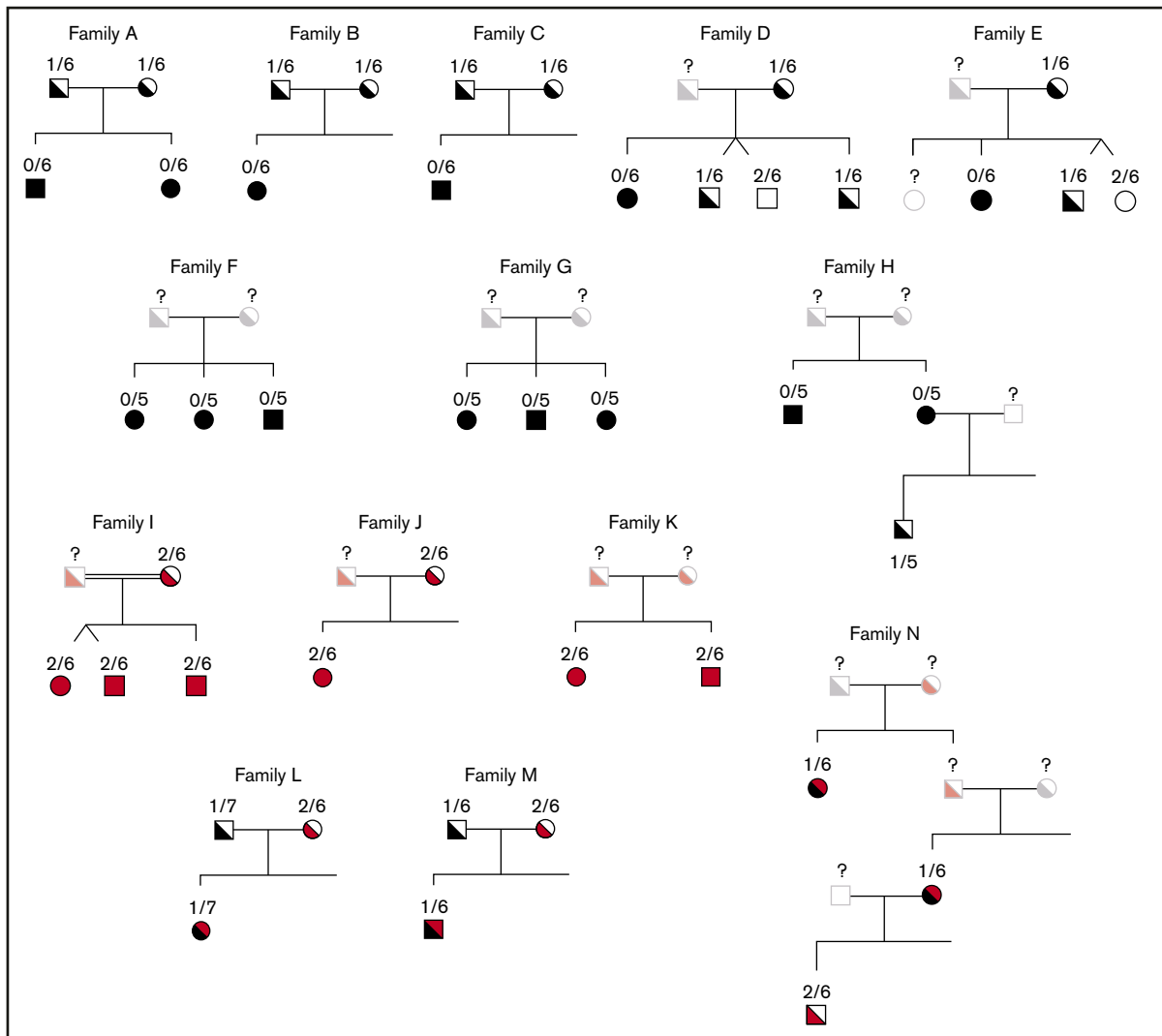


Figure 7. GTGT/ Δ GT CNV in families of patients with $p47^{phox}$ CGD. In the pedigrees presented, the GTGT/ Δ GT genotype is above the individual tested. Symbols in black represent patients and carriers with the Δ GT mutation; symbols in red represent patients and carriers with non- Δ GT mutations; symbols in black and red represent compound heterozygotes with a Δ GT mutation and a non- Δ GT mutation; open symbols represent individuals tested that have a normal phenotype and genotype; faded symbols represent individuals that have not been tested but their phenotype is presumed. Consanguineous marriages are indicated by double lines between pedigree symbols.

We have developed a ddPCR assay that can identify those patients with the Δ GT mutation from patients with other mutations in *NCF1*. An individual with 0 copies of GTGT can be directly diagnosed with $p47^{phox}$ CGD, which is the case in 84% of patients. However, among these 113 patients, the CNV of *NCF1* and its pseudogenes range from 4 to 7, with most individuals having either 5 (17%) or 6 (81%) total copies. Individuals with 1 copy of GTGT can either be carriers of $p47^{phox}$ CGD or $p47^{phox}$ CGD patients who are compound heterozygous for other mutations in *NCF1*. Further testing (DHR, $p47^{phox}$ FACs, and/or immunoblot) is required to differentiate the carriers of $p47^{phox}$ CGD from the patients with $p47^{phox}$ CGD. For 1/6 carriers, 1 copy of *NCF1* carries the common Δ GT mutation, whereas the other copy carries GTGT. If a $p47^{phox}$ CGD patient exhibited 2/6, he/she presumably has distinct mutations elsewhere in *NCF1*.

Both normal subjects and $p47^{phox}$ patients have CNV in *NCF1* and its pseudogenes. Moreover, a significant proportion (16.3%) of

normal subjects ($n = 245$ subjects) have more than 2 copies of *NCF1* containing the GTGT, 36 normal subjects have 3 copies, and 4 normal subjects have 4 copies. Despite increased numbers of wild-type alleles, neither $p47^{phox}$ protein expression nor ROS production is elevated. Most *NCF1* CNV is found within the Caucasian and Hispanic populations.

Recently, De Boer et al¹⁵ reported Ashkenazi Jews in whom both parents carried 3/6 (3 GTGT of 6 *NCF1/NCF1BNCF1C*), including a wild-type *NCF1* on 1 chromosome; on the other chromosome, each parent carried an *NCF1* with a known CGD-causing mutation (c.579G>A, p.Trp193Ter)¹⁹ and a GTGT-containing *NCF1* gene at the position of a pseudogene. Genetic studies on the fetus determined that it had inherited the mutated chromosome from both parents. Presumably, the fetus would carry 4 GTGT/6 *NCF1/NCF1BNCF1C*, inheriting a known dysfunctional mutation in *NCF1*, but also inheriting a GTGT-containing *NCF1* gene with unknown functionality at the position of a pseudogene. Although

predicted to have p47^{phox} CGD, the infant exhibited normal ROS production, suggesting that the third GTGT-containing copy was a functional *NCF1* gene at the position of a pseudogene and produced functional p47^{phox}. Merling et al.²⁰ used a cell line from a p47^{phox} patient with a non-ΔGT mutation in *NCF1* to genetically edit the ΔGT mutation in the pseudogenes, thereby restoring ROS production from the corrected pseudogene. This confirms that repair of the ΔGT is sufficient to transform a p47^{phox} pseudogene into a functional gene.

Our data add complexity of the *NCF1* locus. There can be both increased and decreased CNV among the wild-type gene and the pseudogenes. There also appears to be correction of pseudogenes by GTGT incorporation, although whether a result of duplication or recombination events between the wild-type gene and pseudogenes remains to be determined. The use of “signature” sets of nucleotides to define *NCF1* and its pseudogenes, such as many of those listed in supplemental Table 1, may prove unreliable, as Roos et al.¹⁹ have reported that many of the single nucleotide polymorphisms found in *NCF1* are found in *NCF1B* and *NCF1C* and are thought to have arisen through recombination events between the wild-type gene and the pseudogenes. In addition, another mechanism for gene rearrangement that should be considered is template-driven DNA repair of double-strand DNA breaks. Breaks in DNA within the *NCF1* gene could lead to misalignment of *NCF1* with homologous regions of either *NCF1B* or *NCF1C*, leading to incorporation of *NCF1B* (or *NCF1C*) sequence (including the ΔGT mutation) into *NCF1*. Because this may occur randomly, a break in *NCF1* could be repaired using a pseudogene, incorporating the ΔGT into *NCF1*. Alternatively, a break in *NCF1B* or *NCF1C* could be repaired using *NCF1*, incorporating the GTGT sequence from *NCF1* into the pseudogene, “correcting” the ΔGT mutation in a pseudogene; this mechanism would occur with preservation of the total copy number of *NCF1*, *NCF1B*, and *NCF1C*. Although unequal recombination (unequal crossing over) is still the most likely event for the heterogeneity observed in the CNV of *NCF1* and the pseudogenes, this gene repair hypothesis provides a plausible explanation for the differences in GTGT and ΔGT copy number variation found in the normal population.

In summary, flow cytometry and ddPCR expand the diagnostic repertoire for patients and carriers of p47^{phox} CGD. Our flow

cytometer-based assay for p47^{phox} expression allows rapid quantitative diagnosis of p47^{phox} expression. Our ddPCR assays allow quantitative estimates of the relative number of GTGT and ΔGT copies. In geographic regions (eg, the Middle East and India) in which the frequency of autosomal recessive CGD, especially p47^{phox} CGD, is increased, these assays could have a significant effect on the identification of the phenotype and genotype of patients and, equally important, suspected carriers of p47^{phox} CGD. Finally, these tools clarify our understanding of the inheritance of p47^{phox} CGD, and simultaneously show that the *NCF1* locus is more fluid than previously appreciated.

Acknowledgments

This research was supported in part by the Intramural Research Program of the National Institutes of Health, National Institute of Allergy and Infectious Diseases, and in part with federal funds from the National Cancer Institute, National Institutes of Health, under contract HHSN261200800001E.

The content of this publication does not necessarily reflect the views or policies of the Department of Health and Human Services, nor does mention of trade names, commercial products, or organizations imply endorsement by the US Government.

Authorship

Contribution: D.B.K., A.P.H., and X.W. designed the research; S.K., C.S.Z., S.S.D.R., H.L.M., and S.M.H. cared for patients and arranged for sample collections; D.S., K.L., D.F., P.G., D.W.H., D.A.L.P., and L.M. performed experiments; D.B.K. analyzed the results and made the figures; and D.B.K., A.P.H., H.L.M., S.M.H., X.W., and J.I.G. did ongoing data review, wrote, and edited the manuscript.

Conflict-of-interest disclosure: The authors declare no competing financial interests.

ORCID profiles: D.B.K., 0000-0002-9971-0760; A.P.H., 0000-0001-6841-2122; H.L.M., 0000-0001-5874-5775; J.I.G., 0000-0001-7081-7620.

Correspondence: John I. Gallin, Chief Clinical Pathophysiology Section, Laboratory of Clinical Immunology and Microbiology, National Institute of Allergy and Infectious Diseases, National Institutes of Health, 1 Center Dr, Room 201, Bethesda, MD 20892; e-mail: jig@nih.gov.

References

1. Berendes H, Bridges RA, Good RA. A fatal granulomatosis of childhood: the clinical study of a new syndrome. *Minn Med*. 1957;40(5):309-312.
2. Kuhns DB, Alvord WG, Heller T, et al. Residual NADPH oxidase and survival in chronic granulomatous disease. *N Engl J Med*. 2010;363(27):2600-2610.
3. Bakri FG, Martel C, Khuri-Bulos N, et al. First report of clinical, functional, and molecular investigation of chronic granulomatous disease in nine Jordanian families. *J Clin Immunol*. 2009;29(2):215-230.
4. Fattahi F, Badalzadeh M, Sedighipour L, et al. Inheritance pattern and clinical aspects of 93 Iranian patients with chronic granulomatous disease. *J Clin Immunol*. 2011;31(5):792-801.
5. Rawat A, Singh S, Suri D, et al. Chronic granulomatous disease: two decades of experience from a tertiary care centre in North West India. *J Clin Immunol*. 2014;34(1):58-67.
6. Bridges RA, Berendes H, Good RA. A fatal granulomatous disease of childhood; the clinical, pathological, and laboratory features of a new syndrome. *AMA J Dis Child*. 1959;97(4):387-408.
7. Kuhns DB, Long Priel DA, Chu J, Zarembek KA. Isolation and functional analysis of human neutrophils. *Curr Protoc Immunol*. 2015;111:7.23.1-16.
8. Chanock SJ, Roesler J, Zhan S, et al. Genomic structure of the human p47-phox (*NCF1*) gene. *Blood Cells Mol Dis*. 2000;26(1):37-46.

9. Nunoi H, Rotrosen D, Gallin JI, Malech HL. Two forms of autosomal chronic granulomatous disease lack distinct neutrophil cytosol factors. *Science*. 1988;242(4883):1298-1301.
10. Böyum A. Isolation of mononuclear cells and granulocytes from human blood. Isolation of monuclear cells by one centrifugation, and of granulocytes by combining centrifugation and sedimentation at 1 g. *Scand J Clin Lab Invest Suppl*. 1968;97:77-89.
11. Kuhns DB. Assessment of neutrophil function. In: Rich RR, Fleisher TA, Shearer WT, Schroeder HWJ, Frew AJ, Weyand CM, eds. *Clinical Immunology: Principles and Practice*. 4th ed. London, United Kingdom: Elsevier Saunders; 2013:1183-1191.
12. Köker MY, Sanal O, van Leeuwen K, et al. Four different NCF2 mutations in six families from Turkey and an overview of NCF2 gene mutations. *Eur J Clin Invest*. 2009;39(10):942-951.
13. Wada T, Muraoka M, Toma T, et al. Rapid detection of intracellular p47^{phox} and p67^{phox} by flow cytometry; useful screening tests for chronic granulomatous disease. *J Clin Immunol*. 2013;33(4):857-864.
14. Hayrapetyan A, Dencher PCD, van Leeuwen K, de Boer M, Roos D. Different unequal cross-over events between NCF1 and its pseudogenes in autosomal p47^(phox)-deficient chronic granulomatous disease. *Biochim Biophys Acta*. 2013;1832(10):1662-1672.
15. De Boer M, Gavrieli R, van Leeuwen K, et al. A false-carrier state for the c.579G>A mutation in the NCF1 gene in Ashkenazi Jews. *J Med Genet*. 2018; 55(3):166-172.
16. Brunson T, Wang Q, Chambers I, Song Q. A copy number variation in human NCF1 and its pseudogenes. *BMC Genet*. 2010;11(1):13.
17. Olsson LM, Nerstedt A, Lindqvist A-K, et al. Copy number variation of the gene *NCF1* is associated with rheumatoid arthritis. *Antioxid Redox Signal*. 2012;16(1):71-78.
18. Dekker J, de Boer M, Roos D. Gene-scan method for the recognition of carriers and patients with p47^(phox)-deficient autosomal recessive chronic granulomatous disease. *Exp Hematol*. 2001;29(11):1319-1325.
19. Roos D, Kuhns DB, Maddalena A, et al. Hematologically important mutations: the autosomal recessive forms of chronic granulomatous disease (second update). *Blood Cells Mol Dis*. 2010;44(4):291-299.
20. Merling RK, Kuhns DB, Sweeney CL, et al. Gene-edited pseudogene resurrection corrects p47^{phox}-deficient chronic granulomatous disease. *Blood Adv*. 2016;1(4):270-278.